RESEARCH ARTICLE

{M}acro-
molecular
Chemistry and Physics
www.mcp-journal.de

Check for updates

A Solution-Processable Pristine PEDOT Exhibiting Excellent Conductivity, Charge Carrier Mobility, and Thermal Stability in the Doped State

Philip Schmode, Adrian Hochgesang, Mahima Goel, Florian Meichsner, John Mohanraj, Martina Fried, and Mukundan Thelakkat*

PEDOT:PSS [poly(3,4-ethylenedioxythiophene) polystyrene sulfonate] is a widely used insoluble conducting polymer, which is therefore processed from dispersions. In this work, PEDOT homopolymers (PEDOT-C_6C_8 1 and 2) highly soluble in common solvents like toluene, tetrahydrofuran, and chloroform are synthesized with a high control of molecular weight and low dispersity using Kumada catalyst transfer polymerization of a newly synthesized EDOT monomer carrying a branched alkyl substituent. Pristine PEDOT-C_6C_8 allows the use in accumulation mode transistors with a high charge carrier mobility of 5×10^{-4} cm^2 V^{-1} s^{-1}. Moreover, these polymers can be doped in a controlled fashion, reaching conductivities of 10^{-3} S cm^{-1} at 10 mol% of a dopant, Spiro-MeOTAD(TFSI)$_2$. The doped state is remarkably stable, retaining 80% of the initial value after annealing under nitrogen at 100 °C and being exposed to ambient atmosphere for up to 12 h. During doping, the hole injection barrier decreases and reaches an impressively low value of 130 meV at only 2.5 mol% dopant loading without loss in carrier mobility; as monitored using ultraviolet photoelectron- and impedance spectroscopy. This new design concept leading to highly soluble polymers with well-controlled molecular weights provides solution-processable PEDOT dopable in a well-controlled fashion.

Dr. P. Schmode, A. Hochgesang, Dr. M. Goel, F. Meichsner,
Dr. J. Mohanraj, M. Fried, Prof. M. Thelakkat
Applied Functional Polymers
University of Bayreuth
Universitätsstr. 30, 95440 Bayreuth, Germany
E-mail: mukundan.thelakkat@uni-bayreuth.de
Prof. M. Thelakkat
Bavarian Polymer Institute
University of Bayreuth
Universitätsstr. 30, 95440 Bayreuth, Germany

1. Introduction

π-conjugated semiconducting polymers as well as their doped counterparts called conductive polymers, which show a good charge transport, low oxidation potential, and a high stability of the oxidized state, are of great interest in the field of organic thermoelectrics, solar cells, and in organic bioelectronics.[1–3] The most widely used p-type conducting polymer is PEDOT:PSS [poly(3,4-ethylenedioxythiophene) polystyrene sulfonate], which is commonly processed as a dispersion in water due to its insoluble nature.[4,5] It is mainly transparent (80–95%) within low thickness ranges and exhibits high conductivity of up to 4600 S cm^{-1}, catching up with elemental metals such as mercury (1 × 10^4 S cm^{-1}).[6–8] PEDOT:PSS is a mixture of two ionomers, where PSS has the function of doping the short PEDOT segments and stabilizing their oxidized state. In this mixture, the short PEDOT segments (7–18 units) are surrounded by the PSS chains with a much higher molecular weight, forming a dispersion in solution and a granular structure in thin films.[9] These unique properties predestine PEDOT:PSS for both high-volume applications such as antistatic coatings as well as specialized fields of research on doped polymers like thermoelectrics or organic solar cells.[10–13] However, there is a big demand for soluble undoped PEDOT polymers due to its low oxidation potential and feasibility of processing thin films from solutions. The advantages of doped PEDOT:PSS are overshadowed by drawbacks such as: i) long-term and thermal instability of thin films; ii) limited solubility in organic solvents; and iii) intrinsically conductive nature hampering the use of undoped material in devices requiring a normally off-behavior, for example, accumulation mode organic field effect transistors (OFET).[14,15] This inherent limitation has instigated recent interest in developing suitably substituted PEDOT homopolymers, which are highly soluble in pristine form, processable from solution and more importantly dopable in a controlled and desired fashion for, for example, bioelectronics and thermoelectric applications.[16,17] The key challenge in synthesizing soluble PEDOT homopolymers is

ADVANCED SCIENCE NEWS
www.advancedsciencenews.com

[M]acro molecular
Chemistry and Physics
www.mcp-journal.de

to select suitable substituents guaranteeing solubility, while still maintaining high molecular weights, because unsubstituted PEDOT is insoluble even at a few repeating units. In addition, the useful electrical properties of PEDOT:PSS, for example, high conductivity, should also be achieved in the new PEDOT homopolymers. Incorporating suitable substituents is a viable strategy, which is also shown in other conjugated polymers like poly(3-hexylthiophene) to improve the solubility and processability of the resulting polymer. In low band gap polymers, a common way to increase the solubility is to introduce branched aliphatic side chains.[18] Various approaches to tackle this challenge of making PEDOT polymers soluble were published, ranging from cyclic alkyl-substituted 3,4-ethylenedioxythiophenes (EDOT) and 3,4-propylenedioxythiophenes (PProDOT) over acyclic linear alkyl branched dioxythiophenes to more elaborate polar sidechains such as sulfonates or ethers.[19–23] Caras-Quintero previously published dihexyl-substituted PEDOT homopolymers employing acid-catalyzed transetherification to form the corresponding EDOT monomers, which were subsequently polymerized by electrochemical oxidation.[24] Recently, Pittelli introduced branched (ethylhexyl-) and unbranched (octyl-) alkyl-substituted poly(dioxythiophenes) synthesized by oxidative polymerization using FeCl$_3$, to obtain doped polymers, however suffering from broad polydispersities ($Đ$ = 1.8–3.8).[25] Yet, no report on a controlled polymerization of soluble PEDOT homopolymer was published until Bhardwaj et al. functionalized an ethylenedioxythiophene monomer with a hexyl side chain and used the controlled polymerization technique of Kumada catalyst transfer polymerization (KCTP) to achieve a PEDOT-C$_6$ homopolymer.[26] Nevertheless, they achieved a polymer with low molecular weight of 4 kg mol^{-1}, indicating that the hexyl side chains did not enhance the solubility of the final polymer sufficiently. We introduced branched side chains to overcome this issue and synthesized a new generation of dibrominated EDOT monomer, to obtain a sufficiently high molecular weight and well-controlled PEDOT homopolymer soluble in common organic solvents. A new monomer synthesis route was developed to obtain an EDOT monomer with a branched 2-hexyldecyl (C$_6$C$_8$) side chain. In this study we present highly soluble PEDOT homopolymer having controlled molecular weight, low polydispersity as synthesized in a living fashion, utilizing KCTP. The two resulting highly defined polymers, differing in the polymer chain lengths, were investigated with spectro-electrochemistry measurements to evaluate their electrochemical oxidizability. Furthermore, the charge carrier mobility in accumulation mode OFETs was measured for the pristine samples. The change in work function and hole injection barrier of doped states of PEDOT-C$_6$C$_8$ polymer obtained by adding Spiro-MeOTAD(TFSI)$_2$ dopant were monitored using ultraviolet photoelectron spectroscopy (UPS). The influence of doping on charge carrier mobility was studied using the negative differential susceptance ($-\Delta B$) method, applying impedance spectroscopy experiments.[27] To summarize, our strategy offers a route to synthesize soluble pristine PEDOT polymers with controlled molecular weights, which allow any degree of doping in solution in a well-controlled fashion, and the doped state was found to be remarkably stable, retaining 80% of the initial value for 12 h in ambient atmosphere after annealing under nitrogen at 100 °C.

2. Results and Discussion

In this study, we first synthesized the new polymer PEDOT-C$_6$C$_8$ starting from 3,4-dimethoxythiophene 1 as shown in **Figure 1a**. Detailed synthetic procedures for the substituent are given in the experimental part.[28] A transetherification between 3-hexylundecane-1,2-diol and 3,4-dimethoxythiophene results in EDOT-C$_6$C$_8$ monomer 2 carrying a branched C$_6$C$_8$ side chain. For the use in the Kumada catalyst transfer polymerization, a further dibromination step is necessary, which was accomplished using N-bromosuccinimide in CH$_3$COOH/THF to yield the monomer 3. We chose two different monomer to nickel catalyst ratios [M]$_0$/[Ni(dppp)Cl$_2$] (30/1 and 10/1) to synthesize PEDOT-C$_6$C$_8$ 1 and 2, which should deliver theoretical molecular weights of 3500 and 10500 g mol^{-1}. Furthermore, a study of the polymerization kinetics was conducted in a separate experiment (Figure 1b). We observed a very rapid increase in molecular weight in the first 30 min of the polymerization before the molecular weight levels off indicating a chain-growth mechanism typically found in KCT polymerizations.[29] After the first 30 mins, the polymer chain grows less rapidly reaching almost a plateau after 4 h. To determine the molecular weight distribution and dispersity of PEDOT-C$_6$C$_8$ 1 and 2, we used size exclusion chromatography (SEC) and MALDI–TOF analysis (See **Table 1**, Figure 1c). SEC measurements revealed well-defined monomodal distributed with low dispersities, but the elution with THF using PS calibration resulted in almost identical molecular weights for the two polymers (Figure S2, Supporting Information). However, the difference in molecular weights could be clearly resolved in MALDI-TOF analysis, showing peak molecular weights of 3 (≈9 repeating units) and 10 kg mol^{-1} (≈27 repeating units), respectively (Figure 1c), as expected from the monomer/catalyst ratio. In both MALDI-TOF spectra the molecular weight of the repeating unit (352 g mol^{-1}) could be confirmed for the peak series. The second peak series of the spectra of PEDOT-C$_6$C$_8$ 1 can be attributed to the doubly charged species of the ionized polymer. Commercially available PEDOT:PSS such as Clevios P is composed of high molecular weight PSS chains (400 kg mol^{-1}) and short PEDOT segments of only 1000–2500 g mol^{-1}, which translates to ≈7–18 repeating units.[9] By eliminating PSS (later for doping), we can increase the content of electroactive PEDOT with a high degree of control over the molecular weight. We can deduce two advantages of our approach using a 2-hexyldecyl side chain monomer in PEDOT polymers: i) no copolymerization necessary to achieve sufficient solubility; ii) high degree of control over molecular weight using KCTP; and iii) low polydispersity (Table 1).

Optical properties play a vital role in devices incorporating PEDOT thin films such as organic solar cells, which were assessed consecutively via UV–Vis–NIR spectroscopy. UV–Vis–NIR absorption and emission studies in THF solution reveal, that both polymers exhibit similar vibronically resolved absorption and photoluminescence features, as well as an identical optical bandgap (Figure 1d). The as-synthesized sample PEDOT-C$_6$C$_8$ 1 exhibits absorption at wavelengths higher than 680 nm compared to PEDOT-C$_6$C$_8$ 2, indicating in-situ doping in the former. From the absorption or PL spectra, qualitative information regarding aggregation in solution was deduced. Both polymers
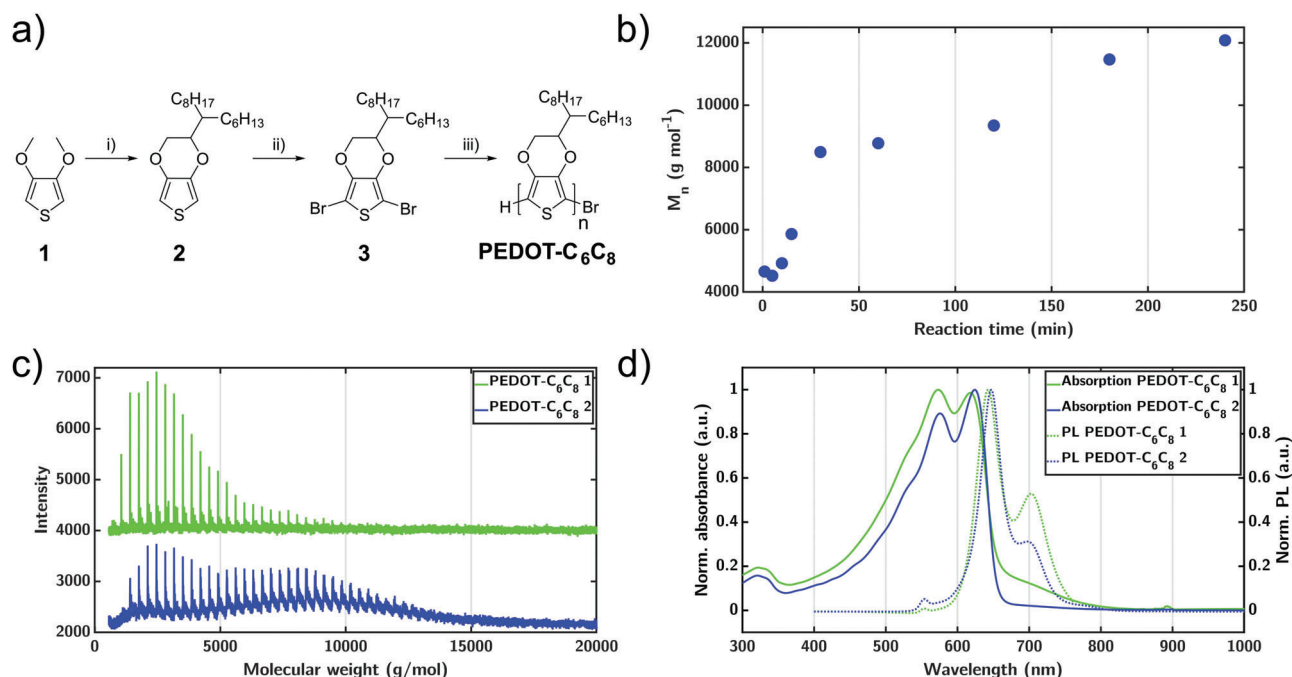
Figure 1. a) Scheme of polymer synthesis for PEDOT-C_6C_8 1 and 2: **i)** 3-hexylundecane-1,2-diol, p-TsOH, toluene, reflux; **ii)** N-bromosuccinimide, CH_3COOH/THF, RT; **iii)** t-BuMgCl, THF, RT, Ni(dppp)Cl$_2$, H$_2$O. b) Kinetic plot of PEDOT-C_6C_8 polymerization with monomer to nickel catalyst ratios $[M]_0$/[Ni(dppp)Cl$_2$] 100:1. M_n determined by SEC using THF as eluent, 1,2-dichlorobenzene as internal reference and narrowly distributed polystyrene standards. c) MALDI-TOF spectra of PEDOT-C_6C_8 recorded with dithranol as matrix. d) UV–Vis absorption and photoluminescence (PL) spectra of PEDOT-C_6C_8 1 and 2 in THF solution, with a polymer concentration of 0.02 mg ml^{-1}.

Table 1. Characteristics of the two synthesized copolymers PEDOT-C_6C_8 1 and 2, determined via SEC, MALDI-TOF, and OFET experiments.

	M_p MALDI-TOF [kg mol^{-1}]	Đ[b]	Repeating units[c]	μ_{hole}[OFET] [cm^2 V^{-1}s^{-1}]
PEDOT-C_6C_8 1	3	1.38	9	1.6×10^{-4}
PEDOT-C_6C_8 2	9.8	1.19	27	5.0×10^{-4}

[a] Dithranol was used as a matrix material, dilution 1:1000; [b] SEC with polystyrene calibration and THF as eluent; [c] Calculated from peak molecular weight determined in MALDI-TOF.

exhibit highly ordered absorption spectra, in which the 0–0 transition peak for both polymers can be distinguished at 638 nm and the 0–1 transition peak at 584 nm, respectively.[30] It can be stated that both PEDOT polymers are highly aggregated in every solvent we tested (chloroform, hexane, THF, etc.). By introducing an aliphatic 2-hexyldecyl side chain, we expect an increased solubility of the pristine PEDOT-C_6C_8 2 homopolymer. To test our hypothesis, we conducted solubility studies, summarized in **Table 2** below.

Pristine PEDOT-C_6C_8 2 offers exceptional solubility of up to 34.1 g L^{-1} in nonpolar, aprotic solvents such as toluene and chlorinated solvents like dichloromethane and trichloromethane. Surprisingly, we were able to dissolve moderate amounts of PEDOT-C_6C_8 even in 1,4-dioxane, ethyl acetate, and hexane. Poor compatibility was found with the highly polar solvents acetonitrile and dimethylformamide. Bu et al. synthesized copolymers of dihexyl-substituted EDOT with the intended aim of high solubility in organic solvents and achieved a solubility of 1.82 g L^{-1} in dichloromethane, affirming the advantages of our homopolymer

design strategy.[31] We investigated the thermal stability of the polymers using thermogravimetric analysis and observed that even the lower molecular weight polymer PEDOT-C_6C_8 1 is stable until 321 °C ($T_{5\%weight loss}$) under nitrogen atmosphere (Figure S3, Supporting Information). PEDOT:PSS on the other hand is prone to thermal decomposition at much lower temperatures, showing multiple degradation steps, namely water loss below 200 °C and PSS degradation at 230 °C before the ultimate oxidation at 420 °C.[32]

The tendency of oxidizability (doping) of both polymers was monitored with spectro-electrochemistry measurements in a three-electrode assembly. Here, we monitored the changes in the absorption spectra of the polymer films in an aqueous NaCl electrolyte when they are subjected to increasing electrochemical doping potentials from 0 to 900 mV in 100 mV steps. The resulting continuous changes in the absorption spectral features and the difference absorption spectra are shown for PEDOT-C_6C_8 2 as an example in **Figures 2**a and b, respectively. Upon applying a doping potential in the range of 300 to 400 mV,

Table 2. Maximum solubilities of PEDOT-C_6C_8 2 in anhydrous organic solvents at RT.

Solvent	Solubility[a] [g L^{-1}]	Solvent	Solubility[a] [g L^{-1}]	Solvent	Solubility[a] [g L^{-1}]
Toluene	34.1 ± 5.20	Trichloromethane	25.1 ± 3.33	Ethyl acetate	0.43 ± 0.15
Dichloromethane	29.9 ± 0.60	1,4-Dioxane	0.67 ± 0.05	Acetonitrile	0.29 ± 0.18
THF	27.0 ± 0.40	Hexane	0.47 ± 0.06	Dimethylformamide	Insoluble[b]

[a] Solubilities determined by preparing a saturated PEDOT-C_6C_8 2 solution in solvent of choice and weighing the mass of the concentrated polymer after evaporation of a known volume of supernatant solution, averaged over three samples; [b] No influence of prolonged heating on solubility was found.
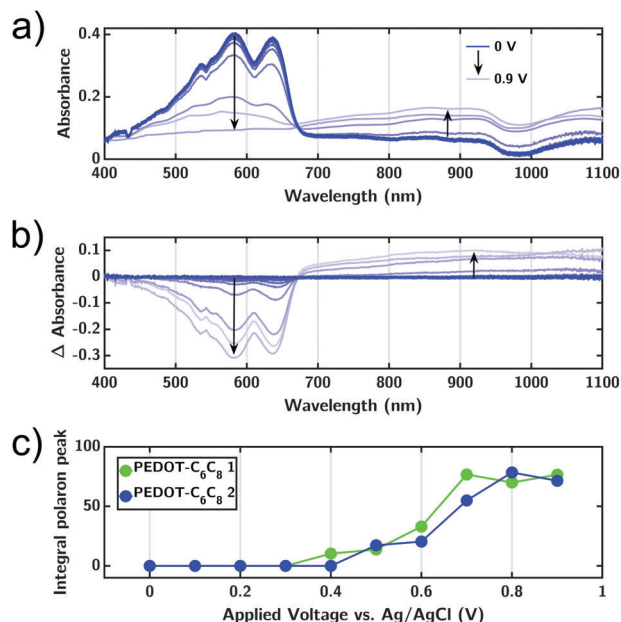

Figure 2. a) Spectro-electrochemistry measurements of thin polymer films on ITO of PEDOT-C_6C_8 2. The spectra were measured in 0.1 M NaCl when the films were biased from 0 to 0.9 V in a three-electrode setup with an Ag/AgCl reference electrode and a Pt counter electrode. −100 mV versus Ag/AgCl was applied prior to SEC measurement for de-doping residual oxidized states. ITO transmittance cut-off below 400 nm is not shown. b) Difference spectra of doped PEDOT-C_6C_8 2 obtained by subtracting the absorption spectra of the polymers in the neutral state (0 V) from the absorption spectra under different applied potentials from 0 to 900 mV. The arrow indicates the direction of spectral changes. c) Correlation of the concentration of polarons indicated by the integrals (obtained by integrating the area under the curve between 680–1100 nm corresponding to the increasing polaron concentration) versus applied potential.

the characteristic polaron absorption between 680 and 1100 nm arises, while concurrently the main $\pi-\pi*$ absorption decreases and finally vanishes completely at 900 mV, which make theses polymers very attractive for transparent electrode applications in the highly doped state (Figure 2a and Figure S3, Supporting Information).[33] The electrochromism of PEDOT-C_6C_8 is comparable to PEDOT:PSS thin films in aqueous solution. In the pristine state, the former offers a larger bandgap (lower absorption onset) and therefore higher transmittance in the visible range than electrochemically de-doped PEDOT:PSS.[34] PEDOT-C_6C_8 1 behaves similarly (data of PEDOT-C_6C_8 1 can be found in Figure S4, Supporting Information). Between our poly-

mers, a small variation is observed in the onset potential values, where PEDOT-C_6C_8 1 shows a lower onset of 300 mV versus Ag/AgCl compared to PEDOT-C_6C_8 2 having an onset of 400 mV (Figure 2c). However, the concentration of the electrochemically doped species saturates at about 700 to 800 mV versus Ag/AgCl for both polymers, indicating that probably the oxidation mechanism and the tendency of oxidation in both polymers are similar.

From the low intensity of the polaron absorption shown in Figure 2, we can expect a low charge carrier density (N_D) of pristine PEDOT-C_6C_8 contrary to PEDOT:PSS, which is typically used in depletion-mode organic field-effect transistors due to its inherently conductive nature. This intrinsic behavior allows PEDOT-C_6C_8 to be used in normally-off accumulation mode OFETs, which is inconceivable for PEDOT:PSS without significant chemical changes to the PEDOT backbone or additional de-doping chemistry.[35] The hole mobilities in pristine state, an important electronic property, of both the polymers in undoped state were investigated in commercially available OFET substrates containing different channel lengths ranging from 10 to 20 μm. By plotting the square root of the drain current I_D versus the gate voltage V_G the hole mobility was calculated (see Equation S1, Supporting Information). Hole mobility values of 1.6×10^{-4} cm^2 V^{-1} s^{-1} (PEDOT-C_6C_8 1, Figure S5, Supporting Information) and 5.0×10^{-4} (PEDOT-C_6C_8 2; Figure S6, Supporting Information) were obtained, with an ON/OFF ratio in the range of 2×10^3 to 9×10^3. Undoped, solution processable EDOT-thiophene alternating oligomers show comparable performance in accumulation mode OFETs with $\mu_h = 6 \times 10^{-4}$ cm^2 V^{-1} s^{-1}.[36] PEDOT-C_6C_8 2, the higher molecular weight polymer with 27 repeating units, shows only a 3 times higher charge carrier mobility compared to the low molecular weight one with nine repeat units. This indicates that the dependence of hole mobility on molecular weight is not very pronounced after about nine repeating units, unlike in many other polythiophenes such as P3HT, where orders of magnitude improvement is observed for high molecular weight samples.[37]

The facile polaron formation upon electrochemical doping indicates good chances of obtaining a conducting polymer via chemical doping akin to acid-doped PEDOT:PSS. To test our hypothesis, we exploited the concept of p-doping through HOMO-HOMO electron transfer by employing Spiro-MeOTAD(TFSI)$_2$ as the p-dopant due to its deep singly occupied acceptor levels. (−5.3 eV, chemical structure shown in **Figure 3**a).[27,38,39] We used this kind of electron transfer doping method due to the high stability of the doped state.[27] PEDOT-C_6C_8 1 (3 kg mol^{-1}) displays slight in situ doped behavior in the pristine state, which could not be chemically de-doped fully by treatment with the reducing agent sodium dithionite. Therefore, PEDOT-C_6C_8 2 was selected
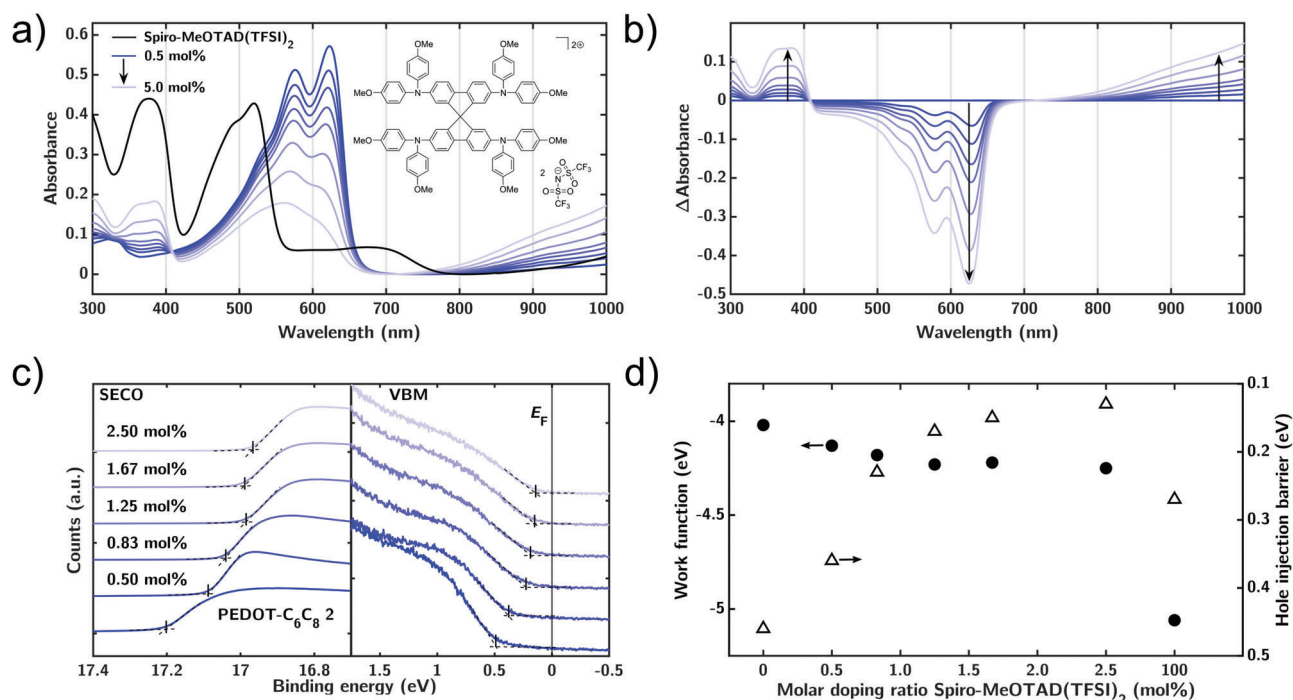
**ADVANCED
SCIENCE NEWS**

www.advancedsciencenews.com

**[M] acro-
olecular
Chemistry and Physics**

www.mcp-journal.de

Figure 3. a) UV–Vis–NIR spectra of 0.02 mg mL^{-1} PEDOT-C$_6$C$_8$ 2 in anhydrous THF doped with Spiro-MeOTAD(TFSI)$_2$. The concentration of Spiro-MeOTAD(TFSI)$_2$ was increased from 0.5 mol% (dark blue) up to 5.0 mol% (faint blue). Absorption spectrum of 100 mol% Spiro-MeOTAD(TFSI)$_2$ referenced in THF (0.01 mg mL^{-1}) is also shown (black). Inset shows the chemical structure of the p-dopant Spiro-MeOTAD(TFSI)$_2$. b) Difference spectra were obtained by subtracting the absorption of the pristine PEDOT-C$_6$C$_8$ 2 reference from the chemically doped polymer solutions. The spectra were recorded under N$_2$ atmosphere in a sealed quartz glass cuvette of 1 cm optical path length. c) UPS measurement of the secondary electron cut-off region (SECO, left) and the valence band maximum (VBM, right) of PEDOT-C$_6$C$_8$ 2 doped with increasing amounts of Spiro-MeOTAD(TFSI)$_2$. d) Workfunction (left y-axis) and hole injection barrier (right y-axis) of pristine PEDOT-C$_6$C$_8$ 2 and Spiro-MeOTAD(TFSI)$_2$ and their mixtures as measured by UPS.

for further chemical doping experiments and for a detailed consequent study of the electronic properties. PEDOT-C$_6$C$_8$ 2 was first investigated to determine the absolute ionization potential and work function in pristine state using UPS. The recorded valence band maximum (VBM) and secondary electron cut-off (SECO) regions of the pristine PEDOT-C$_6$C$_8$ 2 film with respect to E_F are shown in Figure 3c. The onset of the VBM is located 460 meV below E_F. Considering the optical band gap (ca. 1.8 eV) of the polymer, E_F is positioned near to the HOMO, suggesting an intrinsic p-type nature of the polymer. The measured ionization potential (−4.48 eV) emphasizes its shallow HOMO levels, which could facilitate exothermic electron transfer from the polymer HOMO to lower lying unoccupied levels, for example, Spiro-MeOTAD(TFSI)$_2$ HOMO (possibly SOMO) positioned at −5.3 eV, effectively p-doping PEDOT-C$_6$C$_8$. UPS studies by Xing et al. on as-prepared, neutral PEDOT prior to PSS doping revealed a similar HOMO value of −4.7 eV, with a reported work function of −4.0 eV.[40] This similarity excludes effects of the introduced C$_6$C$_8$ side chain on the frontier orbitals, preserving the useful oxidizability of PEDOT:PSS. Further, the change in the electronic levels of PEDOT-C$_6$C$_8$ 2 as a function of dopant molar ratio was monitored through UPS measurements (Figure 3c,d). The measured VBM and SECO regions of PEDOT-C$_6$C$_8$ 2 doped with Spiro-MeOTAD(TFSI)$_2$ up to 2.5 mol% are shown in Figure 3c. With increasing dopant concentration from 0.5 up to

1.25 mol%, E_F continues to shift closer to the VBM of PEDOT-C$_6$C$_8$ 2, decreasing the hole injection barrier; concurrently, SECO also moves towards the lower binding energy region, shifting down the work function value, as typically observed in p-doped systems.[27] These changes are plotted in Figure 3d and the absolute values are collected in Table S7, Supporting Information. Further increase in the dopant concentration up to 2.5 mol% practically coalesce the polymer VBM with E_F, thus reducing the hole injection barrier down to 130 meV. This is an impressive value for a p-type polymer with a remarkably low dopant content (2.5 mol%), which emphasizes the facile and controlled oxidative nature of PEDOT-C$_6$C$_8$, as well the efficient doping ability of Spiro-MeOTAD(TFSI)$_2$.[27]

After assessment of the involved energy levels, which clearly allow for exothermic electron transfer from PEDOT-C$_6$C$_8$ HOMO to Spiro-MeOTAD(TFSI)$_2$ HOMO and evaluating the influence of doping on work function using UPS, we monitored the polaron formation on the polymer by UV–Vis optical spectroscopy during chemical doping. The p-doping process was investigated via a UV–Vis absorption titration experiment, in which aliquot amounts of Spiro-MeOTAD(TFSI)$_2$ were added to a PEDOT-C$_6$C$_8$ 2 solution, and consequent spectral changes were observed, as shown in Figure 3a,b. With increasing dopant concentration, as similar to SEC experiment, a continuous and linear rise in polaron absorption in the range of 680 to 1100 nm
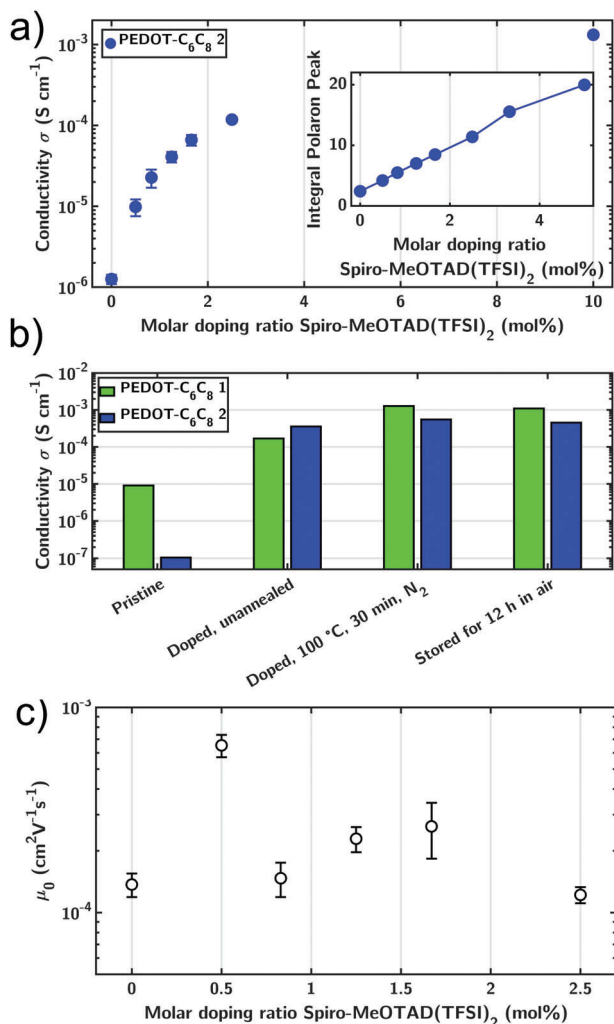
**ADVANCED
SCIENCE NEWS**

www.advancedsciencenews.com

[M] acro-
molecular
Chemistry and Physics
www.mcp-journal.de

Figure 4. a) Thin film conductivities of PEDOT-C_6C_8 2 doped with Spiro-MeOTAD(TFSI)$_2$ as a function of molar dopant ratio with an inset showing the linear correlation between the integral of polaronic peak absorption of the doped polymer solutions (integrated between isosbestic point at 716 and 1000 nm) and the molar percentage of Spiro-MeOTAD(TFSI)$_2$ dopant in solution. b) Electrical conductivity (pristine, doped unannealed, doped annealed at 100 °C under N$_2$ for 30 min and 100 °C, 30 min N$_2$ annealed samples after 12 h storage in air) of PEDOT-C_6C_8 1 and 2, which were doped with 10 mol% of Spiro-MeOTAD(TFSI)$_2$. c) Zero-field mobilities μ_0 of PEDOT-C_6C_8 2 doped with different amounts of Spiro-MeOTAD(TFSI)$_2$ as measured by negative differential susceptance ($-\Delta B$) method on metal-semiconductor devices. The field-free mobilities were obtained by extrapolating log(μ(F)) versus $F^{0.5}$ plots towards the y-intercept.

and concomitant decrease of the neutral main $\pi-\pi^*$ absorptions at 638 and 584 nm were observed. The linear increase of the integral of polaronic peak absorption of the doped polymer solutions (integrated between isosbestic point at 716 and 1000 nm) with the molar percentage of Spiro-MeOTAD(TFSI)$_2$ dopant in solution is given as an inset in **Figure 4**a. In addition a strong feature around 370 nm arises with increasing molar ratio of Spiro-MeOTAD(TFSI)$_2$, possibly originating from the residual or reduced dopant content (Compare the absorption of pure dopant shown as a black curve in Figure 3a).

As UV–Vis–NIR absorption experiments provide clear evidence for polaron formation and UPS studies confirm the gradual shift of the workfunction towards VBM on doping, we conducted conductivity studies on the chemically doped PEDOT-C_6C_8 to assess the influence of doping on conductivity and the stability of the formed polaronic states as shown in Figure 4a,b and Tables S2 to S6, Supporting Information. Sufficient delocalization and mobility of these charge carriers may result in significantly enhanced electrical conductivity. The electrical conductivities of pristine and doped polymers in thin films were measured on as cast and annealed films. Varying the molar ratio of Spiro-MeOTAD(TFSI)$_2$ to PEDOT-C_6C_8 2 reveals a steady increase in conductivity, which asymptotically reaches 1.32 × 10^{-3} S cm^{-1} (Figure 4a). For pristine as-cast films, PEDOT-C_6C_8 1 show the unusual high conductivity value of 10^{-5} S cm^{-1}, which can be explained only due to possible in situ doping via air oxidation. On the other hand, the pristine PEDOT-C_6C_8 2 exhibited an electrical conductivity of 1.04 × 10^{-7} S cm^{-1}. Upon doping with 10 mol% Spiro-MeOTAD(TFSI)$_2$, both polymers gain orders of magnitude in electrical conductivity, precisely PEDOT-C_6C_8 1 to 3.58 × 10^{-4} S cm^{-1} and PEDOT-C_6C_8 2 reaching 1.10 × 10^{-3} S cm^{-1} (Figure 4b). In comparison to other reported PEDOT homopolymers, acid-doped side-chain functionalized PEDOT-S conductivity was reported as 2 × 10^{-4} S cm^{-1} by Cutler et al.[22] Poly(3,4-propylenedioxythiophene) PProDOT doped with the electron acceptor Ni(tfd)$_2$ reached 1.2 × 10^{-3} S cm^{-1}, whereas branched alkyl side-chain PProDOT oxidized with tris(4-bromophenyl)ammoniumyl hexachloroantimonate displays a similar conductivity of ca. 10^{-3} S cm^{-1}, rendering our reported PEDOT-C_6C_8 system highly competitive in the limited chemical space of doped soluble PEDOT homopolymer materials.[17,25] In addition, PEDOT:PSS typically lacks fine tuneability of the electrical conductivity below 1 S cm^{-1} necessary in, for example, hole-transport layers for solar cells, with most reports focussing on post-treatment to induce metal-like conductivities for electrode applications.[7,41,42]

Aside from controlled polymerization, as well as high solubility in a broad range of solvents and tuneable conductivity in films processed from solution, resilience against environmental factors such as oxygen, water, and heat are key requirements for use in commercial applications. To evaluate the thermal stability of our pristine and doped PEDOT-C_6C_8 system, we studied the changes in electrical conductivity in details after: i) heating under inert atmosphere, followed by; ii) heating of the same samples in ambient atmosphere; and iii) after storage at room temperature for 12 h. The annealing protocols and all the conductivity data are summarized in under Tables S3–S6, Supporting Information. First, we annealed stepwise the as-cast polymer films at 100° C up to 30 min under nitrogen atmosphere (Figure 4b). Our measurements indicate that annealing under inert atmosphere marginally enhances the conductivity of doped films, which is in agreement with the high exothermicity found for the p-doping process in UPS experiments. Further, to probe the stability of doped films against humid and oxygen rich environments at elevated temperatures, we further annealed the oxidized films stepwise (30 and 120 min) at 100 °C in air. On annealing in air, an initial minor decrease in conductivity of 14% (PEDOT-C_6C_8 1) and 18% (PEDOT-C_6C_8 2) was observed in the first 30 min, which then stabilizes fully. After all the annealing

steps, on storing the samples for 12 h in air at RT, we could confirm that the conductivity of doped films remains virtually unchanged for both PEDOT-C_6C_8 1 and 2 confirming very high stability of these doped polymers. Contrarily, both pristine polymers display signs of air-doping after prolonged exposure to ambient atmosphere, resulting in enhanced conductivity values compared to as-cast pristine films. Commercially available PEDOT:PSS degrades to ca. 63% of the initial conductivity at 100 °C for 12 h in ambient atmosphere, further highlighting the remarkable stability of our new generation chemically doped PEDOT-C_6C_8 against thermal and environmental factors.[43]

As outlined in our OFET experiments, the electrical mobility μ is not only important in field-effect transistors (according to Equation S1, Supporting Information), but also dictates the electrical conductivity σ together with the charge carrier density N_D and elementary charge e in unipolar (i.e. single carrier type) systems via Equation (1) and consequently influences derived variables, for example, the Seebeck coefficient S in organic thermoelectric materials.[44]

$$\sigma = eN_D\mu \tag{1}$$

Since it is difficult to determine the charge carrier mobility of conducting systems (doped polymers in general) using conventional methods such as OFET or SCLC methods, we determined field dependent charge carrier mobilities of pristine and doped of PEDOT-C_6C_8 2 using negative differential susceptance ($-\Delta B$) method utilizing impedance spectroscopy on metal-semiconductor substrates. A detailed description of this method and the Equations S3 to S7, Supporting Information, used for the calculation of charge carrier mobility are given (Figures S1 and S7, Supporting Information). In Figure 4c, the zero-field charge carrier mobilities of the pristine and doped PEDOT-C_6C_8 2 are plotted versus the dopant concentration.

The measured zero-field mobility μ_0, 1.37×10^{-4} cm^2 V^{-1} s^{-1} for pristine sample (at 0 mol% dopant) is comparable with μ values from OFET measurements ($\mu_{OFET} = 5 \times 10^{-4}$ cm^2 V^{-1} s^{-1}), proving the applicability of the negative differential susceptance ($-\Delta B$) method. Adding 0.5 mol% of Spiro-MeOTAD(TFSI)$_2$ to PEDOT-C_6C_8 2 increases μ_0 by a factor of 4.8 from 1.37×10^{-4} to 6.53×10^{-4} cm^2 V^{-1} s^{-1}, possibly due to trap filling process. Further dopant addition up to 2.5 mol% proves to have no detrimental effect on charge transport, albeit yielding zero-field mobilities comparable to pristine sample, consistent with the doping of highly disordered OSC systems as shown by Arkhipov et al.[45] Field-dependent mobilities of doped PEDOT:PSS were reported to be 4.5×10^{-2} cm^2 V^{-1} s^{-1} in OFET-structures with calculated carrier densities of 10^{20} cm^{-3}.[46] By applying Equation (1) to μ_0 and σ of PEDOT-C_6C_8 at 2.5 mol% Spiro-MeOTAD(TFSI)$_2$, a carrier density of ca. 6×10^{18} cm^{-3} can be estimated. By decreasing N_D, μ is commonly decreased concurrently in organic semiconductors.[47] Taking this relationship into account, PEDOT-C_6C_8 offers a well-balanced mobility at high conductivities. Our study proves chemical p-doping based on HOMO-HOMO electron transfer yields delocalized and mobile charge carriers resulting in an exceptionally stable and highly conductive PEDOT-C_6C_8 system. Table S8, Supporting Information, summarizes the parameters determined with OFET, impedance, and conductivity measurements.

3. Conclusion

In summary, we synthesized a highly soluble, branched alkyl side chain bearing PEDOT homopolymer via controlled Kumada catalyst transfer polymerization. A new monomer synthesis route was developed to obtain a 3,4-ethylenedioxythiophene monomer Br$_2$-EDOT-C_6C_8, carrying branched alkyl chains. MALDI-TOF and SEC measurements revealed well-defined polymers with low polydispersity and molecular weights of up to 10 kg mol^{-1} ($\approx$27 repeating units). Absorption and photoluminescence spectroscopy confirmed a high degree of aggregation in solutions of PEDOT-C_6C_8. In contrast to well-established, intrinsically conductive PEDOT:PSS, we were able to fabricate accumulation mode organic field effect transistors using this PEDOT polymer delivering a promising hole mobility of 5×10^{-4} cm^2 V^{-1} s^{-1}. Furthermore, the ease of PEDOT-C_6C_8 oxidation is explained by spectro-electrochemistry and UPS measurements. On employing the hole conductor salt, Spiro-MeOTAD(TFSI)$_2$ as a p-type dopant for PEDOT-C_6C_8 results in a high conductivity of 1.3×10^{-3} S cm^{-1} for 10 mol% dopant. Deeper insight into the doped states using UPS, UV–Vis–NIR absorption, and impedance spectroscopic measurements highlights the reduced hole injection barrier of oxidized PEDOT-C_6C_8, while conserving its original charge carrier mobility. The doped polymer exhibits a remarkable stability against thermal and environmental factors, retaining a conductivity value of 1×10^{-3} S cm^{-1} after annealing at 100 °C in nitrogen for 30 min and storing in ambient atmosphere for up to 12 h. This outstandingly stable doped state mimicking PEDOT:PSS could help to ease the availability of solution processable conducting polymers. This work opens a new pathway to obtain highly soluble, solution processable PEDOT homopolymers having controlled molecular weights, which are chemically dopable in a desired fashion.

4. Experimental Section

General: Anhydrous solvents with a purity of >99.5% for synthesis and spectroscopical characterization were purchased from Thermo Fisher Scientific. Reagent-grade solvents and reagents for synthesis were supplied by Sigma-Aldrich. All reagents were used without further purification. In the following the synthesis of the branched alkyl substituent and monomer (Scheme S1, Supporting Information), as well as polymer, (Figure 1a) is described.

Synthesis 2-Hexyldecanal: 25 mL DMSO in 620 mL dichloromethane was added to a dry Schlenk flask under nitrogen atmosphere. Thereafter, 12.4 mL (144 mmol, 1.40 equiv.) oxalyl chloride was added at −72 °C and stirred for 30 min. Then, at −72 °C, 25 g (103 mmol) 1,2-hexyldecan-1-ol were added and stirred again for 30 min. Subsequently, 73.8 mL (532 mmol, 5.16 equiv.) NEt$_3$ was added dropwise and reacted at RT for 24 h. 30 ml deionized water was added to the reaction mixture which then was extracted three times with 30 ml of diethyl ether. The organic phase was washed with a 10% HCl solution. Subsequently, the reaction product was washed with a saturated NaHCO$_3$ solution and with a saturated NaCl. The crude product was purified via column chromatography over silica with ethyl acetate:*n*-hexane 1:5. (Yield: 23.1 g, 93%)

^{1}H NMR (300 MHz; ppm, CDCl$_3$, δ_H): 0.88 (t, 6H), 1.14–1.7 (m, 24H), 2.22 (m, 1H), 9.57 (d, 1H).

Synthesis 2-Hexyldecene: 41 g (115 mmol, 1.2 equiv.) methyltriphenylphosphonium bromide was dissolved in 580 mL THF at −78 °C in a dry Schlenk tube under nitrogen. Meanwhile, 12.9 g (114.8 mmol, 1.2 equiv.) potassium *t*-butoxide was dissolved in anhydrous THF and added to the reaction mixture. The mixture was stirred for 1 h at −78 °C.

**ADVANCED
SCIENCE NEWS**

www.advancedsciencenews.com

[M]acro-molecular
Chemistry and Physics

www.mcp-journal.de

23 g 2-hexyldecanal (96 mmol, 1 equiv.) were dissolved in 96 mL THF and slowly added to the mixture at −78 °C and stirred for 1 h. Then, the reaction mixture was allowed to warm up to room temperature and stirred overnight. The mixture was diluted with 250 mL n-hexane and filtered over Celite. The raw product was purified via column chromatography over silica with n-hexane as eluent. (Yield: 14.7 g, 65%)

^{1}H NMR (300 MHz; ppm, CDCl$_3$, δ_H): 0.88 (t, 6H), 1.14–1.42 (m, 24H), 1.94 (s, 1H), 4.88–5.01 (m, 1H), 5.43–5.6 (m, 2H)

Synthesis of 3-Hexylundecane-1,2-diol: The synthesis was done according to Plietker et al. with minor modifications.[28] 18 mL H$_2$SO$_4$ (18.3 mmol, 0.2 equiv.) and 29.4 g NaIO$_4$ (137 mmol, 1.5 equiv.) were dissolved in 60 mL water in a flask and cooled down to 0 °C. An aqueous suspension of 95 mg RuCl$_3$ (0.46 mmol, 0.005 equiv.) in 5 mL water was added slowly to the solution. 274 mL ethyl acetate was added and the suspension was stirred for 5 min. 274 mL acetonitrile were added and the suspension was again stirred for 5 min. 22 g 2-hexyldecene (91 mmol, 1 equiv.) was slowly added and the mixture was stirred for 5 min. The reaction mixture was poured into saturated solutions of 690 mL NaHCO$_3$ and 910 mL Na$_2$S$_2$O$_3$. The organic phase was dried over Na$_2$SO$_4$. The product was purified via column chromatography over silica with n-hexane:ethyl acetate 5:1. (Yield: 9.73 g, 39%)

^{1}H NMR (300 MHz; ppm, CDCl$_3$, δ_H): 0.88 (t, 6H), 1.14–1.42 (m, 24H), 2.01 (s, 1H), 3.50–3.59 (m, 1H), 3.61–3.77 (m, 2H)

*Synthesis of 2-(Pentadecan-7-yl)-2,3-dihydrothieno[3,4-b] [1,4] dioxine - Compound **2***: To a three-necked flask equipped with an argon purge 3,4-dimethoxythiophene **1** (1 g, 6.935 mmol) were added 3-hexylundecane-1,2-diole (3.779 g, 13.87 mmol), p-toluenesulfonic acid monohydrate (0.120 g, 3.467 mmol), and 25 mL anhydrous toluene. The solution was heated at 90 °C for 24 h. After this time, another two equivalents of the diol were added, and the reaction was conducted for another 3 h before it was allowed to cool to room temperature. The reaction mixture was mixed with ethyl acetate and washed twice with a saturated sodium bicarbonate solution. After removal of the solvent, the remaining crude product was isolated by column chromatography (silica gel, n-hexane:dichloromethane 8:2). (Yield: 1.54 g, 63%)

^{1}H NMR (300 MHz; ppm, CDCl$_3$, δ_H): 0.90 (t, 6H), 1.14–1.42 (m, 24H), 1.68 (s, 1H), 3.95–4.03 (m, 2H), 4.06–4.13 (q, 1H), 4.14–4.20 (dd, 1H), 6.31 (s, 2H)

*Synthesis of 5,7-Dibromo-2-hexyl-2,3-dihydrothieno[3,4-b] [1,4] dioxine – Compound **3***: N-bromosuccinimide (1.633g, 9.173 mmol) was dissolved in a mixture of THF (30 ml) and acetic acid (30 ml) and cooled to 0 °C using an ice bath. 2-(pentadecan-7-yl)-2,3-dihydrothieno[3,4-b] [1,4] dioxine **2** (1.54 g, 4.368 mmol) was added against an argon stream dropwise at 0 °C and the solution was stirred at RT for 4 h under the exclusion of light. The solution was then extracted with diethyl ether and washed with water, saturated solution of sodium bicarbonate, and 1 molar solution of sodium hydroxide. The organic phase was dried over anhydrous MgSO$_4$, filtered, and concentrated. The raw product was purified by column chromatography over silica with n-hexane:dichloromethane 8:2 as eluent. (Yield: 1.87 g, 84%)

^{1}H NMR (300 MHz; ppm, CDCl$_3$, δ_H): 0.90 (t, 6H), 1.14–1.42 (m, 24H), 1.68 (s, 1H), 3.95–4.03 (m, 2H), 4.06–4.13 (q, 1H), 4.14–4.20 (dd, 1H)

Synthesis of Poly(2-(pentadecan-7-yl)-2,3-dihydrothieno[3,4-b] [1,4] dioxine) PEDOT-C$_6$C$_8$: 5,7-dibromo-2-hexyl-2,3-dihydrothieno[3,4-b] [1,4] dioxine **3** (1 equiv.) was added to a dry flask under argon and the vessel was evacuated once again and flushed with nitrogen. Then the concentration was set with anhydrous THF to 0.5 mol L^{-1} and t-butylmagnesiumchloride (1.22 M in THF, 0.96 equiv.) was added dropwise. The reaction mixture was stirred for 20 h under the exclusion of light. Then the reaction mixture was diluted with anhydrous THF to 0.1 mol L^{-1}. The respective amount of Ni(dppp)Cl$_2$ (suspension in 2–3 mL anhydrous THF) was added in one portion to start the polymerization. After 4 h the polymerization was quenched with water. The mixture was concentrated, and the polymer was precipitated in methanol. Furthermore, the polymer was purified by Soxhlet extraction with n-hexane, methanol, and chloroform and dried under vacuum.

^{1}H NMR (300 MHz; ppm, CDCl$_3$, δ_H): 0.88 (t, 6H), 1.14–1.42 (m, 24H), 1.94 (s, 1H), 4.01–4.57 (m, 4H)

Conflict of Interest

The authors declare no conflict of interest.

Data Availability Statement

The data that support the findings of this study are available from the corresponding author upon reasonable request.

[1] X. Wu, A. Surendran, J. Ko, O. Filonik, E. M. Herzig, P. Müller-Buschbaum, W. L. Leong, *Adv. Mater.* **2019**, *31*, 1805544.

[2] S. Kee, H. Kim, S. H. K. Paleti, A. El Labban, M. Neophytou, A.-H. Emwas, H. N. Alshareef, D. Baran, *Chem. Mater.* **2019**, *31*, 3519.

[3] B. Vaagensmith, K. M. Reza, M. N. Hasan, H. Elbohy, N. Adhikari, A. Dubey, N. Kantack, E. Gaml, Q. Qiao, *ACS Appl. Mater. Interfaces* **2017**, *9*, 35861.

[4] H. Shi, C. Liu, Q. Jiang, J. Xu, *Adv. Electron. Mater.* **2015**, *1*, 1500017.

[5] W. Lövenich, *Polym. Sci., Ser. C* **2014**, *56*, 135.

[6] J. E. Mccarthy, C. A. Hanley, L. J. Brennan, V. G. Lambertini, Y. K. Gun'ko'ko, *J. Mater. Chem. C* **2014**, *2*, 764.

[7] B. J. Worfolk, S. C. Andrews, S. Park, J. Reinspach, N. Liu, M. F. Toney, S. C. B. Mannsfeld, Z. Bao, *Proc. Natl. Acad. Sci. USA* **2015**, *112*, 14138.

[8] F. C. Walsh, *Trans. IMF* **1991**, *69*, 107.

[9] U. Lang, E. Müller, N. Naujoks, J. Dual, J. Dual, *Adv. Funct. Mater.* **2009**, *19*, 1215.

[10] S. N. Karri, P. Srinivasan, *Mater. Sci. Energy Tech.* **2019**, *2*, 208.

[11] Z. Fan, J. Ouyang, *Adv. Electron. Mater.* **2019**, *5*, 1800769.

[12] R. Yue, J. Xu, *Synth. Met.* **2012**, *162*, 912.

[13] W.-C. Lai, H.-C. Yu, S.-H. Yang, T.-F. Guo, P. Chen, L.-J. Lin, H.-C. Hsu, A. Singh, C.-W. Chu, *Org. Electron.* **2019**, *73*, 266.

[14] M. Hokazono, H. Anno, N. Toshima, *J. Electron. Mater.* **2014**, *43*, 2196.

[15] A. Giovannitti, D.-T. Sbircea, S. Inal, C. B. Nielsen, E. Bandiello, D. A. Hanifi, M. Sessolo, G. G. Malliaras, I. Mcculloch, J. Rivnay, *Proc. Natl. Acad. Sci. USA* **2016**, *113*, 12017.

[16] D. Minudri, D. Mantione, A. Dominguez-Alfaro, S. Moya, E. Maza, C. Bellacanzone, M. R. Antognazza, D. Mecerreyes, *Adv. Electron. Mater.* **2020**, *6*, 2000510.

[17] J. F. Ponder, A. K. Menon, R. R. Dasari, S. L. Pittelli, K. J. Thorley, S. K. Yee, S. R. Marder, J. R. Reynolds, *Adv. Energy Mater.* **2019**, *9*, 1900395.

[18] T. Weller, M. Breunig, C. J. Mueller, E. Gann, C. R. Mcneill, M. Thelakkat, *J. Mater. Chem. C* **2017**, *5*, 7527.

[19] E. E. Havinga, C. M. J. Mutsaers, L. W. Jenneskens, *Chem. Mater.* **1996**, *8*, 769.

[20] P. Das, B. Zayat, Q. Wei, C. Z. Salamat, I.-B. Magdău, R. Elizalde-Segovia, D. Rawlings, D. Lee, G. Pace, A. Irshad, L. Ye, A. Schmitt, R. A. Segalman, T. F. Miller, S. H. Tolbert, B. S. Dunn, S. R. Narayan, B. C. Thompson, *Chem. Mater.* **2020**, *32*, 9176.

[21] J. F. Ponder, B. Schmatz, J. L. Hernandez, J. R. Reynolds, *J. Mater. Chem. C* **2018**, *6*, 1064.

[22] C. A. Cutler, M. Bouguettaya, T.-S. Kang, J. R. Reynolds, *Macromolecules* **2005**, *38*, 3068.

[23] L. R. Savagian, A. M. Österholm, J. F. Ponder, K. J. Barth, J. Rivnay, J. R. Reynolds, *Adv. Mater.* **2018**, *30*, 1804647.

[24] D. Caras-Quintero, P. Bäuerle, *Chem. Commun.* **2004**, 926.

[25] S. L. Pittelli, M. De Keersmaecker, J. F. Ponder Jr, A. M. Österholm, M. A. Ochieng, J. R. Reynolds, *J. Mater. Chem. C* **2020**, *8*, 683.

[26] D. Bhardwaj, Shahjad, S. Gupta, P. Yadav, R. Bhargav, A. Patra, *ChemistrySelect* **2017**, *2*, 9557.

[27] M. Goel, M. Siegert, G. Krauss, J. Mohanraj, A. Hochgesang, D. C. Heinrich, M. Fried, J. Pflaum, M. Thelakkat, *Adv. Mater.* **2020**, *32*, 2003596.

[28] B. Plietker, M. Niggemann, *Org. Lett.* **2003**, *5*, 3353.

[29] R. H. Lohwasser, M. Thelakkat, *Macromolecules* **2011**, *44*, 3388.

[30] S. T. Turner, P. Pingel, R. Steyrleuthner, E. J. W. Crossland, S. Ludwigs, D. Neher, *Adv. Funct. Mater.* **2011**, *21*, 4640.

[31] H.-B. Bu, G. Götz, E. Reinold, A. Vogt, R. Azumi, J. L. Segura, P. Bäuerle, *Chem. Commun.* **2012**, *48*, 2677.

[32] N. Romyen, S. Thongyai, P. Praserthdam, G. A. Sotzing, *J. Mater. Sci.: Mater. Electron.* **2013**, *24*, 2897.

[33] S. Inal, G. G. Malliaras, J. Rivnay, *J. Mater. Chem. C* **2016**, *4*, 3942.

[34] D. G. Harman, R. Gorkin, L. Stevens, B. Thompson, K. Wagner, B. Weng, J. H. Y. Chung, M. I. H. Panhuis, G. G. Wallace, *Acta Biomater.* **2014**, *14*, 33.

[35] J. Fan, S. S. Rezaie, M. Facchini-Rakovich, D. Gudi, C. Montemagno, M. Gupta, *Org. Electron.* **2019**, *66*, 148.

[36] M. Turbiez, P. Frère, M. Allain, C. Videlot, J. Ackermann, J. Roncali, *Chem. - Eur. J.* **2005**, *11*, 3742.

[37] C. R. Singh, G. Gupta, R. Lohwasser, S. Engmann, J. Balko, M. Thelakkat, T. Thurn-Albrecht, H. Hoppe, *J. Polym. Sci., Part B: Polym. Phys.* **2013**, *51*, 943.

[38] U. B. Cappel, T. Daeneke, U. Bach, *Nano Lett.* **2012**, *12*, 4925.

[39] W. H. Nguyen, C. D. Bailie, E. L. Unger, M. D. Mcgehee, *J. Am. Chem. Soc.* **2014**, *136*, 10996.

[40] K. Z. Xing, M. Fahlman, X. W. Chen, O. Inganäs, W. R. Salaneck, *Synth. Met.* **1997**, *89*, 161.

[41] V. M. Le Corre, M. Stolterfoht, L. Perdigón Toro, M. Feuerstein, C. Wolff, L. Gil-Escrig, H. J. Bolink, D. Neher, L. J. A. Koster, *ACS Appl. Energy Mater.* **2019**, *2*, 6280.

[42] P. Sakunpongpitiporn, K. Phasuksom, A. Sirivat, *Polym. Int.* **2021**.

[43] S. Bontapalle, S. Varughese, *Polym. Degrad. Stab.* **2020**, *171*, 109025.

[44] F. Zhang, C.-A. Di, *Chem. Mater.* **2020**, *32*, 2688.

[45] V. I. Arkhipov, P. Heremans, E. V. Emelianova, H. Bässler, *Phys. Rev. B* **2005**, *71*, 045214.

[46] Q. Wei, M. Mukaida, Y. Naitoh, T. Ishida, *Adv. Mater.* **2013**, *25*, 2831.

[47] S. Olthof, S. Mehraeen, S. K. Mohapatra, S. Barlow, V. Coropceanu, J.-L. Brédas, S. R. Marder, A. Kahn, *Phys. Rev. Lett.* **2012**, *109*, 176601.